AIP Journal of Applied Physics

Concentration, chemical bonding, and etching behavior of P and N at the SiO2/SiC(0001) interface

Y. Xu, C. Xu, G. Liu, H. D. Lee, S. M. Shubeita, C. Jiao, A. Modic, A. C. Ahyi, Y. Sharma, A. Wan, J. R. Williams, T. Gustafsson, S. Dhar, E. L. Garfunkel, and L. C. Feldman

Citation: Journal of Applied Physics **118**, 235303 (2015); doi: 10.1063/1.4937400
View online: http://dx.doi.org/10.1063/1.4937400
View Table of Contents: http://scitation.aip.org/content/aip/journal/jap/118/23?ver=pdfcov
Published by the AIP Publishing

JOURNAL OF APPLIED PHYSICS **118**, 235303 (2015)

Concentration, chemical bonding, and etching behavior of P and N at the SiO_2/SiC(0001) interface

Y. Xu,[1,2,a)] C. Xu,[1,3,a)] G. Liu,[1,b)] H. D. Lee,[1,3] S. M. Shubeita,[1,3] C. Jiao,[4] A. Modic,[4]
A. C. Ahyi,[4] Y. Sharma,[4,c)] A. Wan,[5] J. R. Williams,[4] T. Gustafsson,[1,3] S. Dhar,[4]
E. L. Garfunkel,[1,2] and L. C. Feldman[1,3,d)]
[1]*Institute for Advanced Materials, Devices and Nanotechnology, Rutgers University, Piscataway, New Jersey 08854, USA*
[2]*Department of Chemistry and Chemical Biology, Rutgers University, Piscataway, New Jersey 08854, USA*
[3]*Department of Physics and Astronomy, Rutgers University, Piscataway, New Jersey 08854, USA*
[4]*Department of Physics, Auburn University, Auburn, Alabama 36849, USA*
[5]*Evans Analytical Group, East Windsor, New Jersey 08520, USA*

(Received 14 August 2015; accepted 24 November 2015; published online 17 December 2015)

Phosphorous and nitrogen are electrically active species at the SiO_2/SiC interface in SiC MOSFETs. We compare the concentration, chemical bonding, and etching behavior of P and N at the SiO_2/SiC(0001) interface using photoemission, ion scattering, and secondary ion mass spectrometry. Both interfacial P and N are found to be resistant to buffered HF solution etching at the SiO_2/SiC(0001) interface while both are completely removed from the SiO_2/Si interface. The medium energy ion scattering results of etched phosphosilicate glass/SiC not only provide an accurate coverage but also indicate that both the passivating nitrogen and phosphorus are confined to within 0.5 nm of the interface. Angle resolved photoemission shows that P and N are likely situated in different chemical environments at the interface. We conclude that N is primarily bound to Si atoms at the interface while P is primarily bound to O and possibly to Si or C. Different interface passivating element coverages and bonding configurations on different SiC crystal faces are also discussed. The study provides insights into the mechanisms by which P and N passivate the SiO_2/SiC(0001) interface and hence improve the performance of SiC MOSFETs. © *2015 AIP Publishing LLC*.
[http://dx.doi.org/10.1063/1.4937400]

I. INTRODUCTION

Silicon carbide (SiC) is a wide bandgap semiconductor used for power switching and high temperature applications.[1] The most important component in an "all-SiC" power circuit is the 4H-SiC power MOSFET.[2–7] Electronic performance of the device is intrinsically related to the quality of the gate oxide-SiC interface. One widely used fabrication process to reduce the interface trap density in SiC technology is a nitric oxide (NO) anneal.[8–10] An NO (g) anneal after oxidation can significantly reduce the interface trap density, increase the field effect channel mobility, improve oxide reliability, and enhance device performance.[7,9–13] Possible mechanisms by which this anneal affects the SiO_2/SiC interface have been suggested[8] and supported by experimental evidence and theoretical calculations.[14–16] Earlier measurements have shown that N accumulates in a narrow layer ($<$1.5 nm) at the oxide/semiconductor interface[17] with a coverage in the sub-monolayer range.[2,18] Using ultra-high vacuum conditions, an epitaxial interface structure has also been reported.[19–22] These studies indicate that an interfacial layer is formed consisting primarily of nitrogen bonded to three silicon atoms, tying up some of the Si dangling bonds on the Si face.

More recently, improved performance has been achieved by introducing phosphorous to the SiO_2/SiC interface.[3,5,23,24] Phosphorous passivation may be achieved using a phosphosilicate glass (PSG) thin film as the gate dielectric. PSGs are polar dielectrics and their use as a gate dielectric in a device can result in instabilities.[5,23,24] A stabilized P-passivated SiC MOSFET device has been achieved by Sharma *et al.*[3] It was shown that phosphorus is more effective than nitrogen in reducing interface trap density and increasing field effect channel mobility.[3,5,23,24]

In this report, we quantify the areal density and chemical environment of phosphorus at the SiO_2/SiC interface using X-ray photoelectron spectroscopy (XPS), medium energy ion scattering (MEIS), and dynamic secondary ion mass spectrometry (SIMS). The results show that the interfacial P content introduced using the PSG approach contains about 1/3 as many interfacial P atoms as N atoms employing the NO passivation. The interface trap density near the conduction band edge ($E_C - E = 0.2$ eV) is about 60% lower than the trap density in the NO passivated case, and the peak mobility of phosphorus passivated 4H-SiC MOSFET is about twice that of the NO passivated device.[3,5,23,24]

We examine the etching behavior and chemical bonding of phosphorus at the SiO_2/SiC interface and demonstrate

---

[a)]Now at Applied Materials, Inc., Sunnyvale, California 94085, USA.
[b)]Now at Texas Instrument, Inc., Dallas, Texas 75243, USA.
[c)]Now at Dynex Semiconductor Ltd., Lincoln LN2, United Kingdom.
[d)]Author to whom correspondence should be addressed. Electronic mail: l.c.feldman@rutgers.edu

0021-8979/2015/118(23)/235303/5/$30.00

that, similar to interfacial nitrogen,[18,25] the interfacial phosphorus present prior to etching remains after an HF etch. We also present the interfacial P coverage on different crystal faces of 4H-SiC and discuss the chemical environment of interface passivating elements. Accurate P and N contents and depth profiles at the SiO_2/SiC interface are determined using MEIS. Angle resolved XPS analyses for P are compared with the N depth profile at the interface, showing the different bonding configurations of interfacial N and P and supplying further information on their position. Finally, possible mechanisms by which phosphorus improves interface quality and device performance are discussed.

II. SAMPLE PREPARATION

Si-face (4° off-axis) and a-face (on-axis) n-type 4H-SiC samples were cleaned with a standard RCA process. After cleaning, samples underwent dry thermal oxidization at 1150 °C for different times depending on the crystal faces and desired oxide thickness. Samples were annealed in Ar at 1150 °C for 30 min, and then annealed at 1000 °C with a phosphorous containing planar diffusion source (PDS) for various lengths of time. The PDS provides P_2O_5 which diffuses into the thermal oxide and forms PSG.

Nitrogen passivated samples were also prepared for comparison purposes. SiC with 50–60 nm of a dry thermal oxide was exposed to NO at 1175 °C for 2 h, with the flow rate of NO kept at 500 sccm. XPS was performed using a Thermo K-Alpha system with a monochromatic Al Kα source. The Au $4f_{7/2}$ peak, as well as C 1s and Si $2p_{3/2}$ substrate peaks were used for energy referencing. Additional analysis employed SIMS[2] and MEIS.[26] MEIS was carried out using 190 keV helium ions at the Rutgers MEIS facility.[26] MEIS spectra were analyzed to provide total P and N content and to provide a depth profile.

III. PHOSPHORUS ETCHING AT SiO_2/SiC AND SiO_2/Si INTERFACES

Fig. 1(a) shows the SIMS profile of a PSG/SiC sample indicating that the PSG chemical composition is approximately uniform throughout the PSG layer. For comparison, the SIMS profile of a standard NO annealed SiO_2/SiC sample is shown in Fig. 1(b), where N is accumulated exclusively at the interface.

Fig. 2(a) shows the P 2p XPS spectrum from 4H-SiC with ~60 nm PSG grown on the surface, before (black) and after (red) an etch in buffered HF etchant. The PSG chemical composition is approximately the same through the entire oxide layer. The "before etching" samples were partially etched with BOE solution leaving about 5 nm oxide for comparison with fully etched samples. Following etching, a significant amount of P and O is retained at the interface, with a similar atomic ratio as observed in bulk PSG. Fig. 2(b) shows the P 2p XPS spectra before and after etching Si(100) with PSG grown on the surface using the same process as for SiC. The XPS spectrum shows no detectable phosphorous left on the Si surface after HF etching. This etching behavior of P is similar to N on both SiC and Si; both N and P at the SiO_2/SiC interface cannot be completely etched in HF while they can be removed from the Si surface. A "background" XPS spectrum in the Si 2p energy range, taken from a clean Si sample, was subtracted from the experimental data to account for the Si 2p plasmon loss.

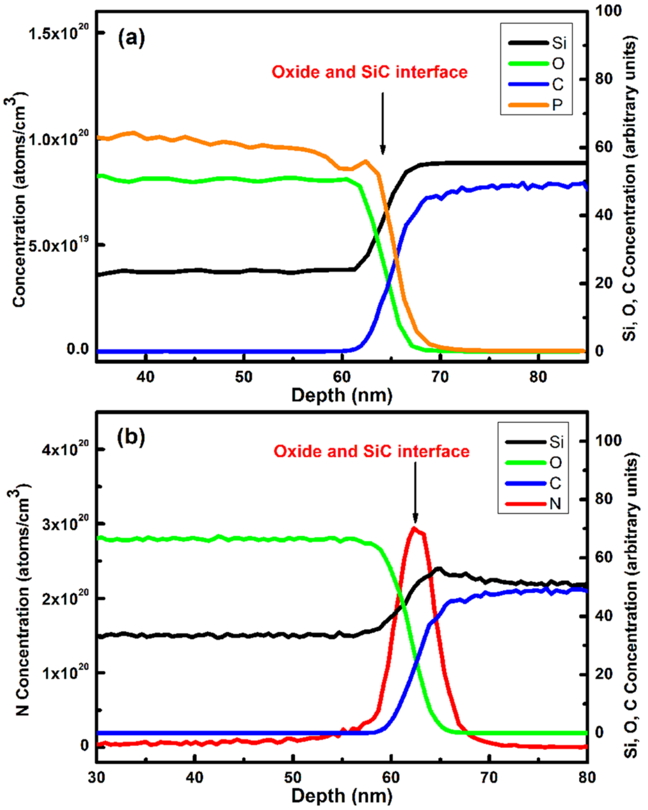

FIG. 1. SIMS profile of (a) a PSG/SiC structure and (b) an NO (g) annealed SiO_2/SiC structure.

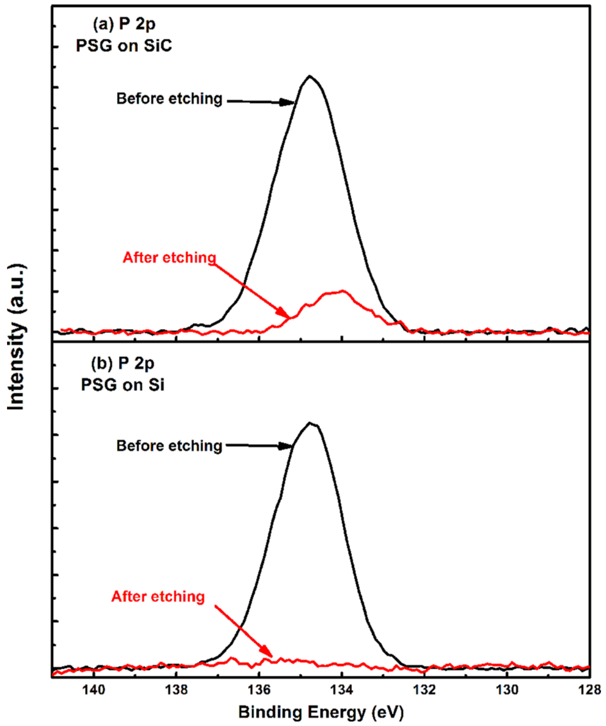

FIG. 2. XPS of P etching at (a) PSG/SiC and (b) PSG/Si interfaces.

IV. PHOSPHORUS BONDING AT THE INTERFACE

Phosphorous is pentavalent, usually bonding to 3, 4, or 5 other atoms in molecules. In bulk PSG, P bonds only with oxygen atoms in the stable PSG network structure.[27,28] Reports list the 2p (XPS) binding energy of P in PSG as between 135–137 eV (depends on the energy reference used).[29] In highly phosphorous doped Si[30] or in phosphorus doped carbon films, the P 2p binding energy is ∼6 eV smaller than that observed in PSG.[31] The P 2p peak of the residual P is shifted only 0.6 eV from the measured PSG value towards a lower binding energy after etching (Fig. 2(a)). This implies that phosphorous atoms at the interface are still primarily bound to oxygen atoms, not silicon. This binding energy shift reflects a slightly different chemical environment for P at the PSG/SiC interface than in the bulk of the PSG. The direction of the shift is consistent with either a secondary nearest neighbor effect, with one of the P atoms being partially bonded to C or Si, or with a change in final state screening as a function of P distance from the interface.[32–34] The different bonding nature in the two P cases may give rise to the higher stability of P at the interface against etching.

V. PHOSPHORUS INCORPORATION AND QUANTIFICATION ON DIFFERENT CRYSTAL FACES

The P coverage on an etched PSG/SiC surface is determined to be 1.2 (±0.2) × 10^{14} atoms/cm^2 based on XPS measurement using the photoelectron mean free path previously reported,[18] and 1.3 (±0.2) × 10^{14} atoms/cm^2 based on MEIS (Fig. 3).

The N 1s XPS peak binding energy and saturation coverage from all three crystal faces are shown in Table I. All the samples were annealed in NO at 1175 °C for 2 h. The C-, a-, and Si-faces of SiC all display a similar N 1s peak shape, and the peak binding energies fall in the range of 397.5–397.9 eV, suggesting that N atoms reside in similar local chemical environments regardless of the exposed crystal face. The detailed bonding of N at the Si-face SiO_2/SiC interface and the nitridation kinetics were reported in two separate papers.[2,18] The current results show that N atoms are also primarily bound to Si atoms on both the C- and a-faces of SiC. The N 1s peak binding energy is 397.5 eV on the Si-face, 397.9 eV on the C-face, and 397.7 eV on the a-face. The small differences of the N 1s binding energies between the different crystal faces may be due to the different Si structure and symmetry on the different crystal faces. Shirasawa *et al.* proposed a structure for the nitrogen containing 6-H Si face grown under different conditions. In the model each interfacial N atom is bound to three Si atoms passivating all the interface dangling bonds.[18,21] Specifically, each N atom bonds to one Si atom from the SiC substrate and two Si atoms from the oxide.[18,21] On the C-face, N atoms have a much higher chance to bond with C atoms from the SiC substrate, and thus slightly shift the N 1s peak towards higher binding energy, which agrees with the N 1s binding energy shift trend from a N-Si bond to a N-C bond. As for the a-face, there are 50% Si atoms and 50% C atoms on the surface, and the binding energy of N lies between that of the Si-face and the C-face, as might be expected.

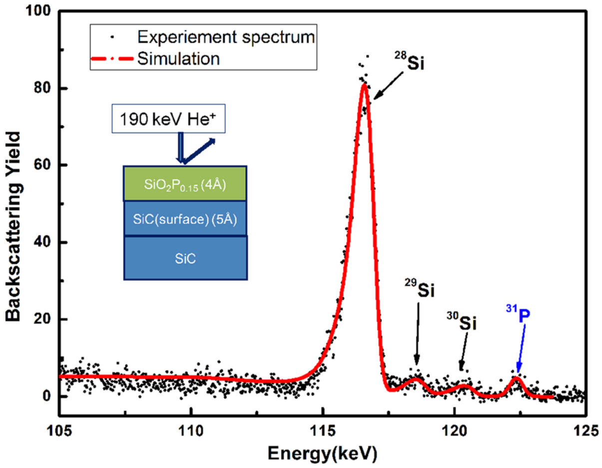

FIG. 3. MEIS spectrum of fully etched phosphorus annealed SiC.

TABLE I. P and N binding energy and saturation coverage on SiO_2/SiC interface (The areal density is calculated using the previously reported photoelectron mean free path, error within ±20%).

	P		N	
Crystal face	BE (eV)	Coverage (10^{14}/cm^2)	BE (eV)	Coverage (10^{14}/cm^2)
C-face	133.5	1.6	398.0	6.7
a-face	133.9	1.2	397.7	6.9
Si-face	134.3	1.1	397.4	4.0
Bulk PSG	134.8			

Similar to N at SiC surfaces,[2,18] P also has different saturation coverages on different crystal faces of SiC. The P 2p XPS binding energy and saturation coverage from all three crystal faces are shown in Table I and compared with the P 2p binding energy from bulk PSG. All three samples were annealed with a P_2O_5 based PDS at 1000 °C for 4 h. The peak binding energies of P on the Si-, C-, and a-faces fall in the range 133.5–134.5 eV, which is 0.6–1.6 eV lower than P from bulk PSG, suggesting that P atoms on all 3 crystal faces are still primarily bound to oxygen atoms which are, themselves, bonded to substrate atoms. The different crystal faces all display similar XPS peak shapes consistent with the notion of similar P bonding on all the faces studied.

Notice that the N and the P XPS peak binding energy shifts on the different crystal faces differ in the extent of their respective shifts: for P, C-face < a-face < Si-face while for N, C-face > a-face > Si-face. Although the reason for this is not fully understood, it suggests that P and N have different bonding environments. This occurs despite the fact that the face dependent coverages roughly follow the same order with lowest coverage on the Si face for both P and N.

VI. PHOSPHOROUS CONCENTRATION PROFILE ACROSS THE SiO_2/SiC INTERFACE

Interfacial phosphorous improves device electrical performance by producing a lower interface trap density and a higher mobility, but with a lower interface coverage, than that of N.[35] Evidently, P is a more efficient passivating agent for interface traps.[3,5,23,24]

Information about the P depth profile at the interface can clarify the role that phosphorus plays at the interface of a SiC device and its relationship to N. MEIS (with ion-channeling) and angle-resolved XPS were used for interface P and N profiling. The MEIS results of etched PSG/SiC (Fig. 3) and etched NO (g) annealed SiC[18] not only provide an accurate coverage but also indicate that both the passivating nitrogen and phosphorus are confined to within 0.5 nm of the interface.

Although MEIS modeling rules out the possibility that P or N atoms are buried deeper than 0.5 nm within the SiC substrate,[18] it is still unclear that if all passivating elements (P or N) sit within the last layer of the oxide or the first layer of SiC. Angle resolved XPS measurements were performed in order to obtain more information about the N and P location.

The depth analysis is realized by examining XPS spectra at different exit angles (the angle between the sample normal and the analyzer). Data were collected with angles from 0° to 75°. As the angle is increased, the photoelectrons collected become increasingly surface sensitive. For example, for normal emission (0°) the 1/e depth for N photoelectron emission is 2.2 nm,[18] while at 75° the value reduces to 0.57 nm. (Although the 1/e length at 75° is 0.57 nm the actual grazing angle dependence of the ratio of intensities of the substrate and the N or P impurity can be fit to better establish the depth position of these species). The angle resolved XPS results from P-passivated and N-passivated SiC were then compared. The intensity ratios of the N 1s peak and P 2p peak relative to the Si 2p at different photo-emission angles are calculated for different depth profile models and are compared with experiment. We define the ratio of the P 2p (or N 1s) peak intensity and the Si 2p peak intensity at 0° emission angle as 1, and compare their change with emission angle.

As shown in Fig. 4, if the passivating agent is buried 0.5 nm into the SiC substrate, the relative peak intensity ratio decreases with increasing angle. The blue curve shows the case for the passivating agent at the surface of the SiC substrate and the relative peak intensity ratio stays constant at different angles, with a slight increase at higher angles. Also shown is the N angle resolved data acquired from an etched NO annealed SiC sample. The fact that the N to Si peak intensity ratio increases with increasing emission angle suggests that the majority of the sub-monolayer amount of N atoms, together with the un-etchable oxygen, sit on top of the SiC substrate. This result agrees with the computational results presented in a separate paper.[18] This interface structure supports a model in which N passivates the interface dangling bond defects. The P angle resolved data from an etched PSG/SiC sample is also shown. Comparing the two curves, it is clear that the P peak intensity is increasing faster than the N peak with increasing emission angle. This indicates that the P atoms are located at a larger distance from the SiC substrate than N. Considering the fact that in the PSG film, P is bound only with O, and that silicon phosphides are very unlikely in the presence of oxygen, it is quite possible that the P-passivated interface consists of O-P-O-Si bonding. If P atoms are not directly bonded to the Si, the mechanism of P passivation may be an indirect one, relieving interface stress and passivating dangling bonds.[31]

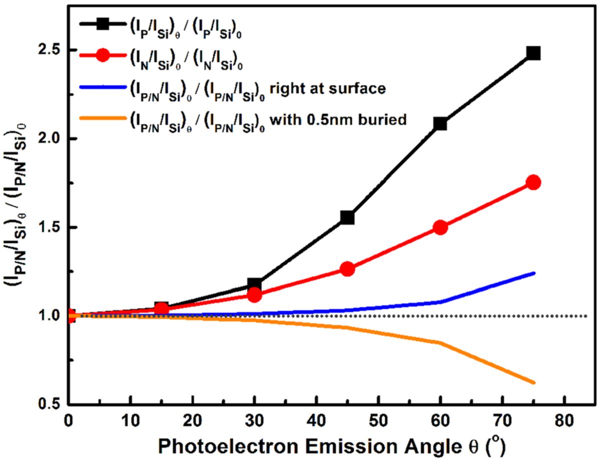

FIG. 4. The peak intensity ratio of P and Si (black) and the peak intensity ratio of N and Si (red) at different photo electron emission angles, the two calculated curves (blue and orange) with passivating element right at surface and at 0.5 nm buried.

VII. RELATIONSHIP OF THESE RESULTS TO THE ELECTRICAL PASSIVATION BEHAVIOR

The total coverage measurements, when correlated to electrical measurement, indicate that P is more efficient than N as a passivating agent. Another, or additional, possible mechanism to explain the observed mobility improvement when using P or N is "counter doping," proposed by Liu *et al.*[4] and Swanson *et al.*[36] In this mechanism a small fraction of the N and P, which are both n-type dopants in SiC, occupy near interface substitutional sites in the SiC substrate, forming a thin surface-doped layer with opposite polarity compared with the p-type MOSFET substrate. This counter-doping model implies the formation of a higher carrier concentration in the inversion mode of the device leading to a higher inversion layer field-effect mobility.

Fiorenza *et al.* reported the doping concentration at the passivated and un-passivated surface using scanning capacitance microscopy,[37] and calculated that the counter doping portion is about 0.03% of the total interfacial N content and 1% of the total interfacial P content, equivalent to $1.2 \times 10^{11}/\text{cm}^2$ N atoms or $1.1 \times 10^{12}/\text{cm}^2$ P atoms[37] based on our total coverage measurements. The fact that the active counter dopant ratio is 30 times higher for P than for N, and 10 times greater in absolute number, makes the counter-doped P content consistent with the experimental result that P-passivated devices have more free electrons and higher electron density,[38] result in a higher field effect mobility with lower total P content.[4] Note that the counter doping P or N concentration would be only a small portion of the total interfacial content, well below the detection limit of most direct physical analysis methods.

VIII. SUMMARY

For the P-passivated SiO_2/SiC interface created via the PSG process, phosphorous is found to be bonded to oxygen at the interface as well as in the bulk SiO_2 (PSG) layer. Both P and O remain after an HF etch of the dielectric on all SiC surfaces, but are completely removed on Si surfaces. The etching behavior of P is similar to that observed for interfacial N on both SiC and Si surfaces. Angle resolved XPS and MEIS suggest that the majority of P atoms sit above the SiC substrate bound to O, and appear not to be directly bonded to the SiC substrate. Both N and P reduce the interface defect state density, while a small portion may enter the SiC substrate and act as an n-type counter dopant.[4]

ACKNOWLEDGMENTS

The authors would like to thank the support of U.S. Army Research Laboratory (Contract No. W911NF-07-2-0046, Dr. Aivars Lelis, TPC), and the II-VI Foundation Block-gift program Cooperative Research Initiative. The authors also acknowledge the support of National Science Foundation (Grant No. DMR-0907385) under the direction of Professor S. T. Pantelides. C. Xu, H. D. Lee, and T. Gustafsson acknowledge the support of the National Science Foundation (Grant No. DMR-1106070).

[1] J. A. Cooper, M. R. Melloch, R. Singh, A. Agarwal, and J. W. Palmour, IEEE Trans. Electron Devices **49**, 658 (2002).
[2] Z. Chen, Y. Xu, E. L. Garfunkel, L. C. Feldman, T. Buyuklimanli, W. Ou, J. Serfass, A. Wan, and S. Dhar, Appl. Surf. Sci. **317**, 593 (2014).
[3] Y. K. Sharma, A. C. Ahyi, T. Isaacs-Smith, A. Modic, M. Park, Y. Xu, E. L. Garfunkel, S. Dhar, L. C. Feldman, and J. R. Williams, IEEE Electron Device Lett. **34**, 175 (2013).
[4] G. Liu, A. C. Ahyi, Y. Xu, T. Isaacs-Smith, Y. K. Sharma, J. R. Williams, L. C. Feldman, and S. Dhar, IEEE Electron Device Lett. **34**, 181 (2013).
[5] Y. K. Sharma, A. C. Ahyi, T. Issacs-Smith, X. Shen, S. T. Pantelides, X. Zhu, L. C. Feldman, and J. R. Williams, Solid-State Electron. **68**, 103 (2012).
[6] X. Zhu, A. C. Ahyi, M. Y. Li, Z. J. Chen, J. Rozen, L. C. Feldman, and J. R. Williams, Solid-State Electron. **57**, 76 (2011).
[7] J. Rozen, A. C. Ahyi, X. G. Zhu, J. R. Williams, and L. C. Feldman, IEEE Trans. Electron Devices **58**, 3808 (2011).
[8] H. F. Li, S. Dimitrijev, H. B. Harrison, and D. Sweatman, Appl. Phys. Lett. **70**, 2028 (1997).
[9] G. Y. Chung, C. C. Tin, J. R. Williams, K. McDonald, M. Di Ventra, S. T. Pantelides, L. C. Feldman, and R. A. Weller, Appl. Phys. Lett. **76**, 1713 (2000).
[10] G. Y. Chung, C. C. Tin, J. R. Williams, K. McDonald, R. K. Chanana, R. A. Weller, S. T. Pantelides, L. C. Feldman, O. W. Holland, M. K. Das, and J. W. Palmour, IEEE Electron Device Lett. **22**, 176 (2001).
[11] G. Y. Chung, J. R. Williams, C. C. Tin, K. McDonald, D. Farmer, R. K. Chanana, S. T. Pantelides, O. W. Holland, and L. C. Feldman, Appl. Surf. Sci. **184**, 399 (2001).
[12] G. Y. Chung, C. C. Tin, J. R. Williams, K. McDonald, M. D. Ventra, S. T. Pantelides, L. C. Feldman, and R. A. Weller, in *Wide-Bandgap Electronic Devices* (Mater. Res. Soc. Symp. Proc., 2000), Vol. 622.
[13] S. Dimitrijev, P. Jamet, and P. Tanner, J. Appl. Phys. **90**, 5058 (2001).
[14] A. J. Lelis, D. Habersat, R. Green, A. Ogunniti, M. Gurfinkel, J. Suehle, and N. Goldsman, IEEE Trans. Electron Devices **55**, 1835 (2008).
[15] D. P. Ettisserry, N. Goldsman, A. Akturk, and A. J. Lelis, J. Appl. Phys. **116**, 174502 (2014).
[16] J. Rozen, S. Dhar, S. K. Dixit, V. V. Afanas'ev, F. O. Roberts, H. L. Dang, S. Wang, S. T. Pantelides, J. R. Williams, and L. C. Feldman, J. Appl. Phys. **103**, 124513 (2008).
[17] K. C. Chang, Y. Cao, L. M. Porter, J. Bentley, S. Dhar, L. C. Feldman, and J. R. Williams, J. Appl. Phys. **97**, 104920 (2005).
[18] Y. Xu, X. Zhu, H. D. Lee, C. Xu, S. M. Shubeita, A. C. Ahyi, Y. Sharma, J. R. Williams, W. Lu, S. Ceesay, B. R. Tuttle, A. Wan, S. T. Pantelides, T. Gustafsson, E. L. Garfunkel, and L. C. Feldman, J. Appl. Phys. **115**, 033502 (2014).
[19] F. Devynck, Z. Sljivancanin, and A. Pasquarello, Appl. Phys. Lett. **91**, 061930 (2007).
[20] P. Kruger, B. Baumeier, and J. Pollmann, Phys. Rev. B **77**, 085329 (2008).
[21] T. Shirasawa, K. Hayashi, S. Mizuno, S. Tanaka, K. Nakatsuji, F. Komori, and H. Tochihara, Phys. Rev. Lett. **98**, 136105 (2007).
[22] T. Shirasawa, K. Hayashi, H. Yoshida, S. Mizuno, S. Tanaka, T. Muro, Y. Tamenori, Y. Harada, T. Tokushima, Y. Horikawa, E. Kobayashi, T. Kinoshita, S. Shin, T. Takahashi, Y. Ando, K. Akagi, S. Tsuneyuki, and H. Tochihara, Phys. Rev. B **79**, 241301(R) (2009).
[23] D. Okamoto, H. Yano, T. Hatayama, and T. Fuyuki, Appl. Phys. Lett. **96**, 203508 (2010).
[24] D. Okamoto, H. Yano, K. Hirata, T. Hatayama, and T. Fuyuki, IEEE Electron Device Lett. **31**, 710 (2010).
[25] H. F. Li, S. Dimitrijev, D. Sweatman, H. B. Harrison, P. Tanner, and B. Feil, J. Appl. Phys. **86**, 4316 (1999).
[26] X. Zhu, H. D. Lee, T. Feng, A. C. Ahyi, D. Mastrogiovanni, A. Wan, E. Garfunkel, J. R. Williams, T. Gustafsson, and L. C. Feldman, Appl. Phys. Lett. **97**, 071908 (2010).
[27] P. Balk and J. M. Eldridge, Proc. IEEE **57**, 1558 (1969).
[28] J. Eldridge and D. D. Kerr, J. Electrochem. Soc. **118**, 986 (1971).
[29] A. Tilocca, Phys. Rev. B **76**, 224202 (2007).
[30] W. B. Ying, Y. Mizokawa, Y. B. Yu, Y. Kamiura, M. Iida, and K. Kawamoto, Appl. Surf. Sci. **100**, 556 (1996).
[31] M. Rusop, X. M. Tian, S. M. Mominuzzaman, T. Soga, T. Jimbo, and M. Umeno, Sol. Energy **78**, 406 (2005).
[32] K. Z. Zhang, K. E. Litz, M. M. B. Holl, and F. R. McFeely, Appl. Phys. Lett. **72**, 46 (1998).
[33] K. Z. Zhang, J. N. Greeley, M. M. B. Holl, and F. R. McFeely, J. Appl. Phys. **82**, 2298 (1997).
[34] Y. Tu and J. Tersoff, Phys. Rev. Lett. **84**, 4393 (2000).
[35] K. McDonald, R. A. Weller, S. T. Pantelides, L. C. Feldman, G. Y. Chung, C. C. Tin, and J. R. Williams, J. Appl. Phys. **93**, 2719 (2003).
[36] L. K. Swanson, P. Fiorenza, F. Giannazzo, A. Frazzetto, and F. Roccaforte, Appl. Phys. Lett. **101**, 193501 (2012).
[37] P. Fiorenza, F. Giannazzo, M. Vivona, A. La Magna, and F. Roccaforte, Appl. Phys. Lett. **103**, 153508 (2013).
[38] D. B. M. Klaassen, Solid State Electron. **35**, 961 (1992).